Blocked polyisocyanates containing monofunctional polyhedral oligomeric silsesquioxane (POSS) as crosslinking agents for polyurethane powder coatings

ARTICLE *in* PROGRESS IN ORGANIC COATINGS · JANUARY 2013

Impact Factor: 2.36 · DOI: 10.1016/j.porgcoat.2012.08.008

1 AUTHOR:

Barbara Pilch-Pitera
Rzeszów University of Technology
17 PUBLICATIONS **125** CITATIONS

SEE PROFILE

Progress in Organic Coatings 76 (2013) 33–41

Contents lists available at SciVerse ScienceDirect

Progress in Organic Coatings

journal homepage: www.elsevier.com/locate/porgcoat

Blocked polyisocyanates containing monofunctional polyhedral oligomeric silsesquioxane (POSS) as crosslinking agents for polyurethane powder coatings

Barbara Pilch-Pitera*

Faculty of Chemistry, Department of Polymer Science, Rzeszów University of Technology, 35-959 Rzeszów, Poland

ARTICLE INFO

Article history:
Received 15 March 2012
Received in revised form 7 August 2012
Accepted 10 August 2012
Available online 10 September 2012

Keywords:
Polyisocyanate
POSS
Polyurethanes
Coatings

ABSTRACT

Blocked polyisocyanate crosslinkers for powder coatings were synthesized using alicyclic diisocyanates (TMDI and IPDI), formic acid, (methylaminopropyl)hepta(isobutyl)Si_8O_{12} (POSS), ε-caprolactam, dibutyltin dilaurate as well as triethylamine as catalysts. The chemical structures of these compounds were characterized by means of IR, ^{1}H NMR and ^{13}C NMR spectroscopy. The three-dimensional surface topography and surface chemical structure of the resulting powder coatings were investigated by using confocal microscope and ATR FT-IR. The values of surface roughness parameters were calculated. The surface topography was correlated with the chemical structure of the coatings and macroscopic surface behaviour: surface free energy, abrasion resistance, hardness, adhesion to the steel surface and impact resistance. Thermogravimetric analysis was employed to assess the hardening property of powder coatings and the thermal decomposition processes.

1. Introduction

In recent years there has been growing interest in organic–inorganic hybrid polymers. It is possible to obtain such polymers for instance by incorporating inorganic groups into the chains of organic polymers. The inorganic components applied for this purpose include polyhedral oligomeric silsesquioxanes (POSS) [1–5]. Polyhedral silsesquioxanes comprise a large group of compounds built of trifunctional silicate units, with the proportion of one atom of silicon to one and a half atom of oxygen ($[RSiO_{3/2}]_n$). In this formula "R" stands for any organic substituent or an atom of hydrogen, while "*n*" most frequently adopts the following values: 6, 8, 10 or 12. In order to build POSS molecules into the polymer chain, it is necessary to synthesize compounds containing R substituents ending with various functional groups, e.g. hydroxyl, epoxy, vinyl or amino. Depending on how many of the R substituents contain reactive functional groups, POSS molecules can be incorporated into the polymer chain as a node of the polymer network, as a part of the main chain, or side chains. Oligomeric silsesquioxanes have been used for modifying such organic polymers as: polypropylene [6], cellulose acetate [7], polyester/cotton blends [8], polyamide [9], and polyurethane [10,11].

Products of this kind combine properties of organic polymers with typical qualities of inorganic compounds. In comparison with traditional polymers their most significant advantages include: reduced combustibility, thermal conductivity, heat emission during combustion and increased hydrophobicity, chemical resistance, mechanical strength, abrasion resistance, and hardness, temperature of thermal decomposition [12,13]. Due to their unique qualities polymers of this type can be applied in various domains. They can be used for instance to obtain coating films with enhanced resistance to external factors [14–16]. Introduction of POSS particles into polyurethane coatings results in their improved performance properties, such as increased hydrophobicity, abrasion resistance and chemical resistance [17].

In this paper I would like to report a convenient way of synthesizing POSS-containing blocked polyisocyanate, which allows for an easy and accurate approach to prepare polyurethane powder coating systems. The synthesis of these polyisocyanates covered four stages: the synthesis of ureaisocyanate, biuret formation, POSS addition and the blocking reaction. Spectroscopic techniques such as Fourier transform infrared spectroscopy (FTIR) and nuclear magnetic resonance spectroscopy (^{1}H NMR and ^{13}C NMR) were used in order to characterize the chemical structure of these polyisocyanates. POSS particles containing one amine group were built into the structure of polyisocyanates to form side chains, which facilitates migration towards the air/film interface to minimize the interfacial energy.

This paper focuses on the results of the study aimed at determining the impact of POSS particles on the properties of polyurethane powder coatings. Confocal microscopy (CLSM) was employed for visualizing the surface topography of obtained coatings. In addition to the surface topography measurements, ATR FT-IR was used to reveal chemical structure at the surface. In order to examine

* Tel.: +48 17 86 51700; fax: +48 17 85 43655.
E-mail address: barbpi@prz.edu.pl

0300-9440/$ – see front matter © 2012 Elsevier B.V. All rights reserved.
http://dx.doi.org/10.1016/j.porgcoat.2012.08.008

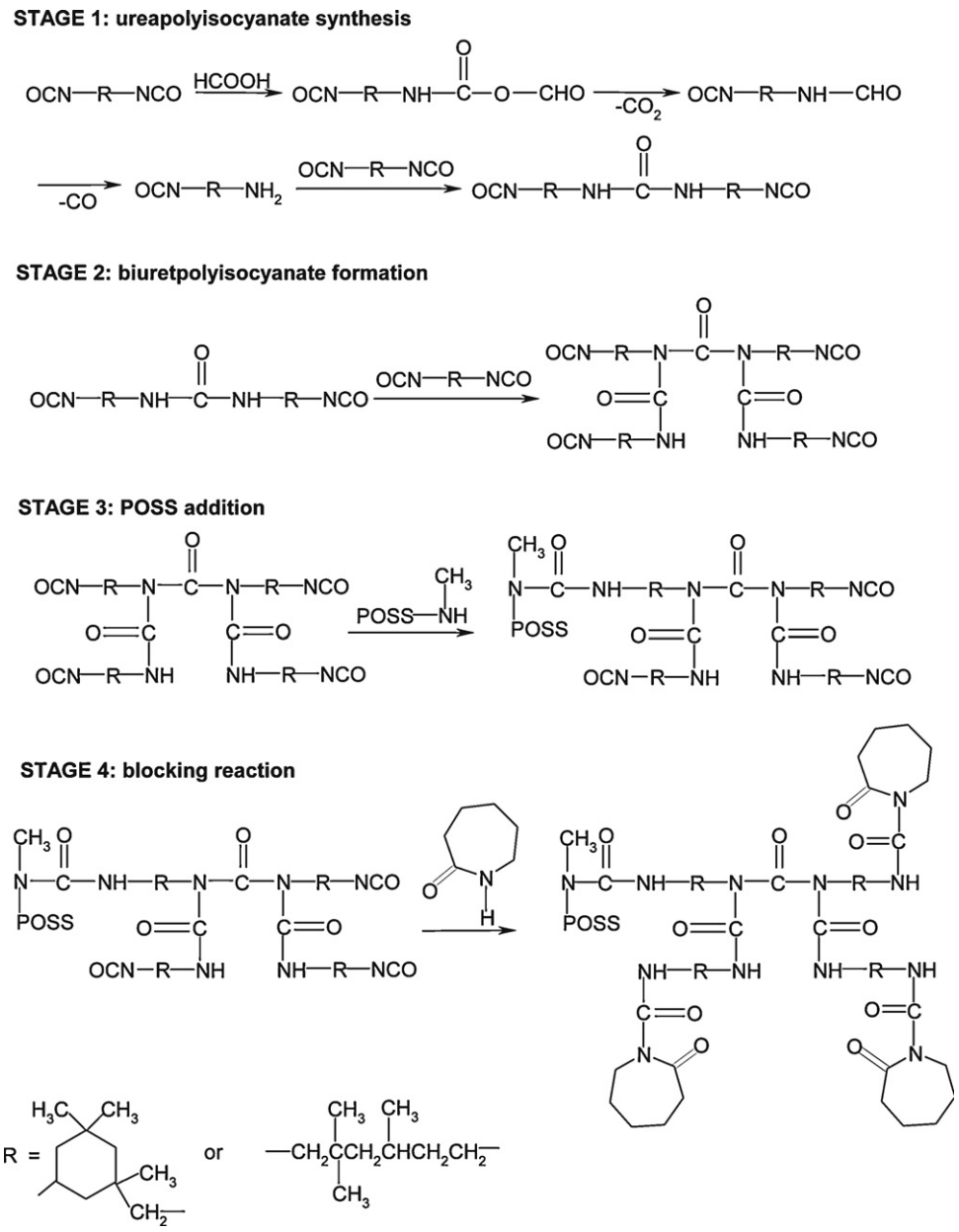

Fig. 1. The reaction scheme of the synthesis.

the way the presence of POSS particles impacts the properties of polyurethane powder coatings, the author carried out the measurements of the contact angle with the liquids: diiodomethane and water, abrasion resistance, hardness, adhesion to the steel surface and impact resistance. Thermogravimetric analysis was applied to assess powder coatings in terms of their hardening property as well as their thermal decomposition process. The relationship between coating properties and POSS content was discussed.

2. Experimental

2.1. Raw materials and reagents

Isophorone diisocyanate (IPDI) – Desmodur I from Bayer A.G. (Leverkusen, Germany). 2,2′,4- and 2,4,4′-trimethyl-1,6-hexamethylene diisocyanate (TMDI) – Vestanat TMDI from Evonik Degussa G.m.b.H. (Marl, Germany). (Methylaminopropyl)hepta(isobutyl)Si_8O_{12} (POSS) from Hybrid Plastics (Hattiesburg, USA). ε-Caprolactam (C) from Zakłady Azotowe w Tarnowie – Mościcach S.A. (Tarnów, Poland). Benzoin from Aldrich (Buchs, Switzerland). Rucote 102 (RU) – polyester resin based on isophthalic acid and neopenthyl glycol, acid value: 11–14 mgKOH/g, hydroxyl value: 35–45 mgKOH/g, T_g: 59 °C, from Bayer A.G. (Leverkusen, Germany). WorleeAdd 902 (acrylate resin), Resiflow PH-240 (polyacrylic resin adsorbed on silica) and WorléeAdd ST-70 (stannous octoate (II)) from Worlée – Chemie G.m.b.H (Lauenburg, Germany).

2.2. Synthesis of POSS containing blocked polyisocyanates

The synthesis covered four stages: synthesis of ureaisocyanate, synthesis of biuretpolyisocyanate, POSS addition and blocking reaction.

2.2.1. Synthesis of ureaisocyanate

Diisocyanate and dibutyltin dilaurate as well as triethylamine as a catalysts (both at 0.1 wt% with respect to diisocyanate) were

Table 1
Qualitative/quantitative components of the polyisocyanates and the powder coatings.

Symbol of IC	POSS content in PIC, wt%	Symbol of PIC	The components content in powder coatings, wt%			Symbol of coating
			PIC	POSS	RU	
TMDI	0	TMDI/C	24.2	0	75.8	TMDI/RU
TMDI	4.1	TMDI/4.1%POSS/C	24.4	1.5	75.6	TMDI/1.5%POSS/RU
TMDI	9	TMDI/9.5%POSS/C	25.0	3.5	75.0	TMDI/3.5%POSS/RU
TMDI	15.8	TMDI/15.8%POSS/C	25.5	6	74.5	TMDI/6%POSS/RU
IPDI	0	IPDI/C	23.5	0	76.5	IPDI/RU
IPDI	4.2	IPDI/4.2%POSS/C	24.3	1.5	75.7	IPDI/1.5%POSS/RU
IPDI	11.6	IPDI/11.6%POSS/C	26.3	4.5	73.7	IPDI/4.5%POSS/RU
IPDI	18.5	IPDI/18.5%POSS/C	27.2	7.5	72.8	IPDI/7.5%POSS/RU

placed in a three-necked flask equipped with a reflux condenser, thermometer, glass stirrer, nitrogen inlet and dropping funnel. A calculated amount of formic acid (to keep the molar ratio of diisocyanate to formic acid at 4:1) was introduced drop-wise to diisocyanate. The time of introduction was adjusted to 30 min. The reaction mixture was then maintained at the temperature of 75 °C, stirred and refluxed for 3 h in the case of TMDI, and for 6 h in the case of IPDI diisocyanate. The end point of the reaction was controlled by the content of –NCO groups.

2.2.2. Biuretpolyisocyanate synthesis

The reaction mixture was heated up to 140 °C, stirred and refluxed for 12 h in the case of TMDI, and 26 h in the case of IPDI ureaisocyanate.

2.2.3. POSS addition

A calculated amount of POSS was added to reaction mixture in each case (the amount of POSS was selected in such a way as to make sure that its content in the coating was within the range 1.5–7.5%).

2.2.4. Blocking reaction

A calculated amount of the blocking agent (ε-caprolactam) was added to reaction mixture in each case (the molar ratio of –NCO group to blocking agent at 1:1). The reactions were carried out in THF at the temperature of 65 °C for 3 h in the case of TMDI, and for 6 h in the case of IPDI biuret. The products were evaporated under vacuum and dried at the temperature of 100 ± 1 °C to remove the solvent. The reaction scheme characterizing all steps of the synthesis was presented in Fig. 1. The obtained products were marked with symbols, where individual segments stand for the names of the feeds used: e.g., IPDI/4.2%POSS/C is made from IPDI, POSS as well as ε-caprolactam, and contains 4.2%POSS.

2.3. Preparing powder compositions and coatings

The blocked polyisocyanate was mixed with polyester resin RUCOTE 102 (NCO:OH molar ratio = 1:1) as well as catalyst WorleeAdd ST-70 (stannous octoate(II)) (0.5 wt%), flow control agent Resiflow PH-240 (3 wt%) and degasing agents: WorleeAdd 902 (1.5 wt%) and benzoin (1 wt%). The mixture was grinded, melted and pulverized to the average particle size of 60 μm. The final powder coating was applied manually to steel panels and cured at 180 °C for 30 min. The obtained powder compositions were marked with symbols, where individual segments stand for the names of the feeds used: e.g., TMDI/1.5%POSS/RU contains TMDI, 1.5%POSS and polyester resin Rucote102 (Table 1).

2.4. Measurements

2.4.1. Characterisations of polyisocyanates

2.4.1.1. Concentration of –NCO groups. The typical dibutylamine method was employed. Excess of unreacted dibutylamine was titrated with aqueous HCl against bromophenol blue [18].

2.4.1.2. Structural analysis. FT-IR spectroscopy: The IR spectra were taken by means of Thermo Scientific Nicolet 6700 FT-IR spectrophotometer, in KBr pellets.

^{1}H NMR and ^{13}C NMR spectroscopy: The NMR spectra were recorded using a Bruker Avance^{II} 500 MHz unit. Deuterated chloroform, $CDCl_3$, or dimethylsulfoxide DMSO-d_6, were used as solvents. The chemical shifts values are given in ppm with reference to internal tetramethylsilane.

2.4.2. Characterisations of powder coatings

2.4.2.1. Surface topography measurements. The surface topography of the powder coatings was investigated with the use of a NanoFocus Confocal Microscope (CM) μsurf explorer with a capability to perform an accurate three-dimensional measurement and submicron imaging, with outstanding 2 nm resolution. The 505 nm diode combined with optics, specifically enables resolution in *z*-direction 2–20 nm as well as in *x*, *y*-direction 500–3100 nm. The negative values on *z*-scale stand for the levels of valley depths, whereas the positive values define valley height from the mean line.

The values of Ra, Rz, Rt, Rq, Rmax, Rms S. and Rpc were used to characterise the coating roughness parameter. These symbols are defined as follows:

Ra arithmetic mean deviation of the assessed profile,
Rz max. height of the profile within a sampling length,
Rq root mean square deviation of the assessed profile,
Rms S. root-mean-square slope of the profile within a sampling length. The result is expressed in degrees.
Rpc peak count, number of peaks per centimetre. Each peak being higher than the upper threshold, and falling under the lower threshold. The threshold is defined by a band, symmetrically separated (Sep) around the mean line (if Sep = 0.5 μm, then the size of side of the mean is ±0.25 μm). The result is expressed in peaks/cm.

2.4.2.2. ATR FT-IR spectroscopy. Attenuated total reflection (ATR) spectra were recorded by reflection technique with a Thermo Scientific Nicolet 6700 FTIR instrument, equipped with a diamond crystal. The ATR experiment involves placing the sample to be analysed in contact with a high refractive index material (diamond, $n = 2.3$) through which the infrared beam is confirmed.

2.4.2.3. Determination of surface free energy (SFE). Surface free energy (γ_S), is quantified using a contact angle goniometer made by Cobrabid-Optic. Diiodomethane and water were chosen as immersion liquids. Measurements were performed at 22 ± 1 °C. Surface free energy (SFE) was determined taking into account the measured contact angles for the coatings, by means of Owens–Wendt method [19].

2.4.2.4. Thermogravimetric analysis (TGA). The thermal performance of the powder coatings was investigated with the use of Mettler Toledo TGA/DSC1 differential calorimeter with the Star^e System software. The instrument was calibrated with the use of *In* standard. The samples (0.002 g) were placed in alumina crucibles. These were weighed to the nearest 0.000001 g and placed in the measuring chamber. The progressive heating was initiated at the rate of 10°/min. and the temperature was gradually increased from 25 °C to 500 °C. The DTA, TG and DTG curves were recorded. The measurements were taken in the environment of nitrogen which was passed at the rate of 50 cm^3/min.

2.4.2.5. Thickness. The thickness of the coatings was determined by means of the magnetic method in accordance with EN ISO [20]. The measurement was performed with an electronic gauge designed for measuring coating thickness on ferromagnetic substrate, and equipped with probe including cable; directly before the measurement the instrument was calibrated on unpainted substrate using the attached thickness models.

2.4.2.6. Abrasion resistance. Abrasion resistance of the coatings was determined by means of Gardner Tester in accordance with PN [21]. In order to determine the value, the coating in question was exposed to the action of free falling abrasive material passing through a pipe of 19 mm in diameter. The applied abrasive material was noble electro-corundum (white aluminium oxide) with the grain size of 0.5–0.8 μm. Abrasion resistance was expressed as a ratio of the applied abrasive material mass [kg] to the thickness of the coating in question [μm].

2.4.2.7. Hardness. Relative hardness of the coatings was determined by means of König Pendulum manufactured by BYK, in accordance with PN-EN ISO [22]. The examined panel was located on the pendulum table with the coating facing up. After the pendulum was set on the panel it was displaced at the angle of 6° and set in motion. The time in which the amplitude of the oscillations decreased to 3° was measured. Relative hardness of the coating was determined as the ratio of the time of decreasing oscillations of a pendulum supported on the examined coating to the time of decreasing oscillations of a pendulum supported on a polished glass plate.

2.4.2.8. Adhesion to the steel surface. Coatings were assessed for their surface adhesion by means of cross-cut test in accordance with PN-EN ISO [23]. The coatings were incised into the substrate with a multi-cut tool equipped with 6 cutters with the spacing of 2 mm, manufactured by Byk. Then the coatings were incised at the angle of 90° in relation to the first incisions to create a network. A soft brush was moved back and forth a few times along the network diagonals. The surface of incision network was examined with naked eye and classified on 0–5 six-point scale. The best surface adhesion is in the case of coatings classified with 0 score, whose incision edges are completely smooth, and the worst adhesion is marked with 5, in this case the damaged surface of the incision network exceeds 65%.

2.4.2.9. Impact resistance. The measurements were performed with rapid deformation test by means of a falling weight of 1 kg with indenter of 10 mm in diameter in accordance with PN-EN ISO [24]. The weight was fastened in a vertical tubular guide with graduation. The examined panel was placed with the painted side facing up, on a steel element with a hole of 16.3 mm diameter located centrally under the indenter. Subsequently, the weight was released to fall onto the indenter. The impacted spots were assessed for cracks using magnifying glass. The assumed test result was the ultimate height, expressed in centimetres, from which the falling weight did not damage the coating.

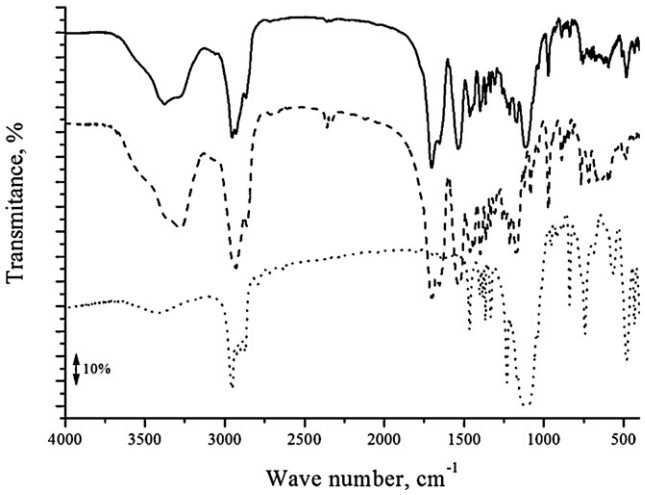

Fig. 2. IR spectra for sample IPDI/18.5%POSS/C (—), POSS (···) and IPDI/C (– – –).

3. Results and discussion

Aliphatic (TMDI) and alicyclic diisocyanates (IPDI) were employed in the syntheses because the coatings produced there from offer high resistance to yellowing. The synthesis itself consisted of four stages (Fig. 1). During the first stage ureaisocyanate was formed in the reaction of diisocyanate with formic acid. In course of this process, initially mixed anhydride of carbamic and formic acid was formed, which after heating to temperature of 75 °C emitted CO_2 producing formamide. Formamide disintegrated with emission of carbon oxide and producing amine-isocyanate. A reaction of amine-isocyanate and diisocyanate generated ureaisocyanate. Biuret formations were generated by adding subsequent particles of diisocyanate to ureaisocyanate. This process required significantly higher temperature (140 °C) and more time. The addition of aliphatic TMDI occurred significantly faster (12 h) than was the case with cycloaliphatic IPDI (26 h). Higher reactivity of TMDI in comparison with IPDI was also noted in the process of addition to urethane bond [25]. During the third stage POSS particle was added. The final stage was designed to block the remaining –NCO groups with the use of ε-caprolactam, which was non-toxic and which could be unblocked at temperature about 170 °C. The synthesis reactions allowed for obtaining products with solid consistency which could be easily powdered.

The progress of subsequent synthesis stages was monitored by analysing the content of free –NCO groups and by comparing the obtained results to those calculated theoretically.

3.1. FT-IR and NMR spectra

The structures of the obtained products were confirmed by FT-IR (Fig. 2) and NMR spectra (Figs. 3 and 4). IR spectra of the investigated polyisocyanates showed wide bands in the range of approx. 1710 cm^{-1} and 3330 cm^{-1}. The first of these represents valence vibrations of carbonyl groups C═O, the second of imine groups, which constitute urea and biuret formations. The amide II band originated from combined scissoring deformation vibrations of the —N—H group occurring at 1540 cm^{-1}. Other amide bands were visible at 1230 cm^{-1} (amide III band), 660 cm^{-1} (amide IV band) and 750 cm^{-1} (amide V band). In the spectrum of polyisocyanate modified with POSS, III, IV and V amide band overlap with bands originating from POSS. Si—O—Si formation absorbs at the

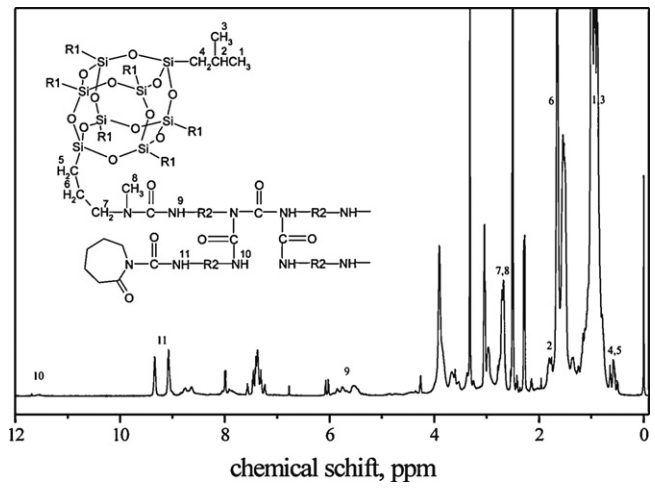

Fig. 3. ^{1}H NMR spectrum for sample IPDI/18.5%POSS/C.

range of 1120 and 840 cm^{-1}, and Si—C at 480 cm^{-1} [26,27]. These signals were visible in the spectrum of both POSS and polyisocyanate modified with POSS. On the other hand, at the range of approx. 2260 cm^{-1} no bands originating from isocyanate groups were found, which confirms the fact of their complete conversion; similarly at the range of approx. 2130 cm^{-1} there were no bands originating from vibrations of carbodiimide groups and at approx. 1415 cm^{-1} from isocyanurate rings generated as by-products. The absence of these bands confirms the proposed route for the reaction.

In ^{1}H NMR spectra the signals coming from biuret and urea bond protons were present at 11.6 ppm (biuret) and 9.3 ppm, 9.1 ppm, 5.4–6.1 ppm (urea), respectively (Fig. 3) [28,29]. The occurrence of double signals originating from biuret and urea groups results from the fact that they can be formed by both the primary and the secondary isocyanate group present in IPDI [30]. At 7.4 ppm a signal originating from NH group of unreacted ε-caprolactam was found. However, it was not necessary to purify synthesized polyisocyanates, as ε-caprolactam evaporates during the coating hardening process. The signals coming from POSS methyl and methylene group protons adjacent to the urea or biuret groups (assigned at 7 and 8) were visible at 2.7 ppm. The shift in the signals in comparison with POSS spectrum (occurring at approx. 2.4 and 2.6 ppm) towards the higher ppm values indicates that POSS particles have been successfully incorporated into the structure of polyisocyanates. The bands at 3.9 ppm and 3.0 ppm come from hydrogen atoms of metin and methylene group of IPDI adjacent to an biuret and urea bond, respectively. Signals of the methyl and methylene groups were found within the range of 0.5–1.9 ppm.

The ^{13}C NMR spectrum (Fig. 4) reveals the presence of new signals in the carbonyl region. The signals originate from the atoms of carbon in carbonyl groups producing urea (154.5 ppm and 153.1 ppm) and biuret (176.8 ppm) bonds as well as from ε-caprolactam carbonyl group (179.4 ppm). The possible dimer (uretdione), trimer (isocyanurate) and carbodiimide of isocyanate would have been present around 157.5, 148.0 and 140.0 ppm, respectively. Such groups were not observed in this case. There were no peaks at 124 ppm, where a characteristic signal of the carbon atom forming an isocyanate group occurs, which shows that diisocyanate was completely converted, something which was also confirmed by the IR analysis. New bands at 75.6, 68.1, 66.9, 53.6 and 46.6 ppm can be seen in the spectra. They originate from carbon atoms of IPDI metin and methylene groups as well as methyl and methylene groups of POSS (assigned at 7 and 8) adjacent to the biuret and urea bond. These signals were shifted towards the lower values of the magnetic field as compared to IPDI and POSS spectra. Within the 43.3–21.8 ppm range carbon atoms creating the IPDI, POSS and ε-caprolactam skeleton generate their characteristic signals.

3.2. Three-dimensional surface topography

To understand the influence of POSS nanoparticles on the final coating structure, the top surfaces of the prepared composites were observed with CLSM. The three-dimensional topographies of powder coatings were shown in Fig. 5. The surface of the POSS-containing powder coating exhibits a slightly larger irregularity and roughness. The values for surface roughness were calculated on the basis of confocal images. The obtained roughness parameters: Ra, Rz, Rq, Rms S. and Rpc were somewhat higher in this case for the POSS-containing sample, than for the TMDI/RU system (Table 2). An increase in the roughness of the coatings is found to coincide with

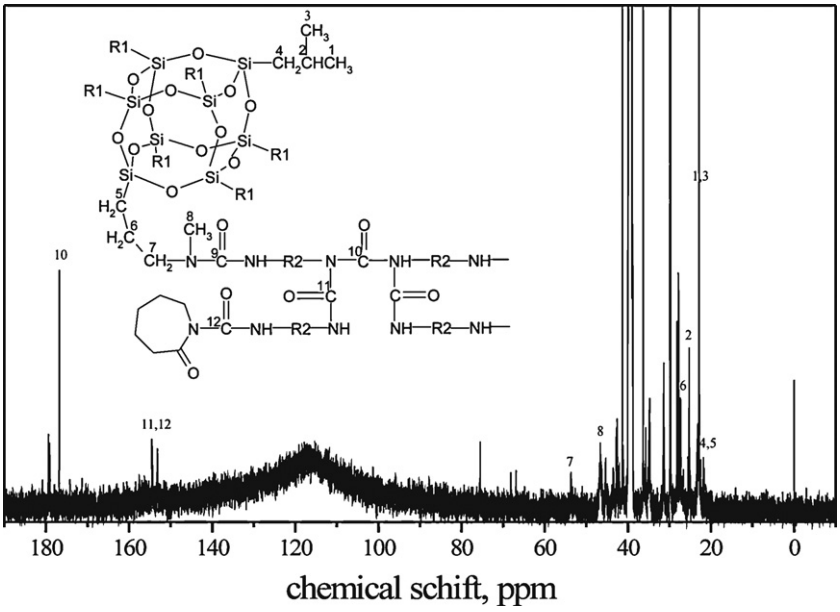

Fig. 4. ^{13}C NMR spectrum for sample IPDI/18.5%POSS/C.

Table 2
Specifications of the coatings performance properties.

Symbol of coating		TMDI/RU	TMDI/1.5%POSS/RU	TMDI/3.5%POSS/RU	TMDI/6%POSS/RU
Water contact angle	Θ [deg]	93.7	96.5	106.0	111.1
Roughness parameters	Ra [μm]	0.238	0.480	0.565	1.046
	Rz [μm]	1.297	2.766	2.812	4.344
	Rq [μm]	0.311	0.446	0.689	1.275
	Rms S. [deg]	0.023	0.032	0.036	0.055
	Sep [μm]	0.5	0.5	0.5	0.5
	Rpc [peak/cm]	0.000	17.573	25.049	25.049
Thickness EN ISO 2808	[μm]	85.0	88.2	71.4	53.2
Adhesion to the steel surface PN-EN ISO 2409	–	0	0	0	0
Hardness PN-EN ISO 1522	–	0.75	0.70	0.68	0.67
Impact resistance PN-EN ISO 6272	The minimum height of the weight fall [cm]	50	50	40	50

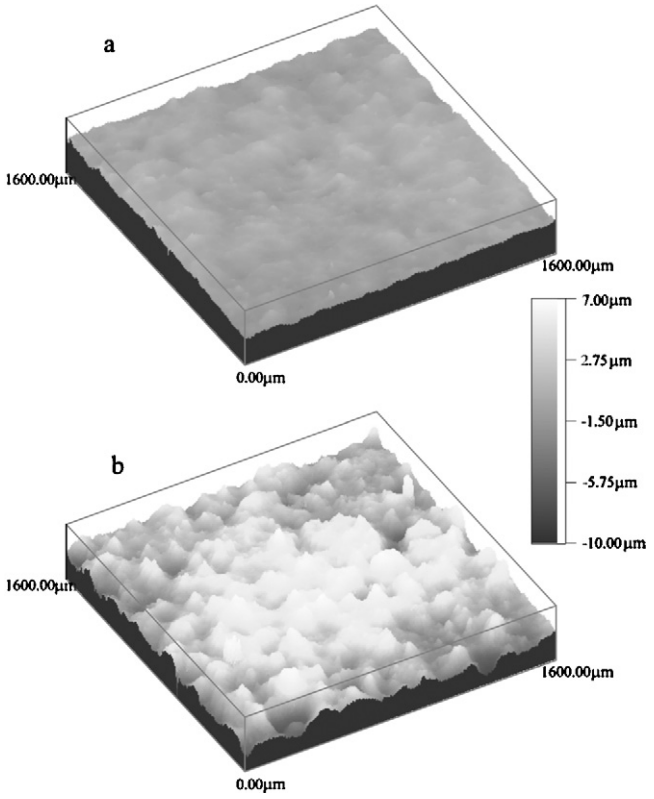

Fig. 5. The confocal laser scanning microscope images of powder coating TMDI/RU (a) and TMDI/6%POSS/RU (b).

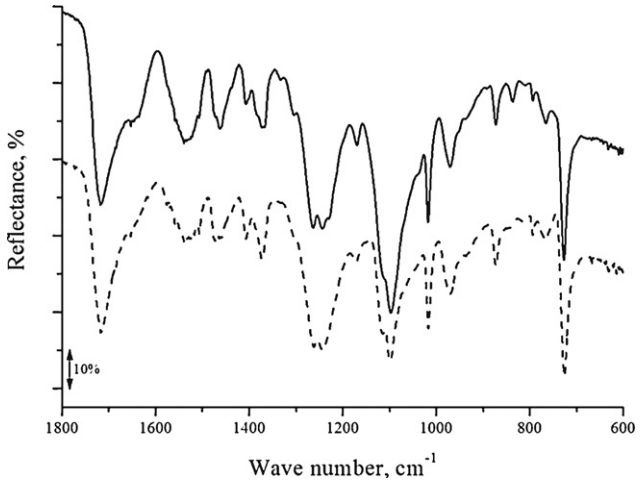

Fig. 6. The ATR FT-IR spectra of the powder coating IPDI/7.5%POSS/RU (—) and IPDI/RU (···).

the growing POSS content. This increase in the surface roughness can be explained with microphase separation with granular-type POSS aggregation on the surfaces of the coatings. The heterogeneous morphology of the coatings revealed the incompatibility of the hydrophobic POSS molecule with the PU matrix. Because of the thermodynamic incompatibility of the POSS and PU components in the matrix, the POSS molecule aggregated on the surfaces of the coatings [11]. The microphase-separated morphology led to very attractive properties of coatings with built-in POSS; these will be discussed below.

3.3. ATR FT-IR spectroscopy

Reflection infrared spectra of IPDI/RU and IPDI/7.5%POSS/RU coatings have been reported for comparison in Fig. 6. The broad bands at 3330 cm^{-1} were assigned to NH stretching vibration of urea and biuret groups (invisible in Fig. 10). The C=O stretching vibrations of urea, biuret and ester groups were responsible for the bands observed at 1715 cm^{-1}. Weak broad bands at 1540 cm^{-1} and 1640 cm^{-1} were connected to C—C ring stretching vibration of polyester resin which included phtalic acid. The N—H scissors deformation vibration and C—N stretching vibration (amide II band) were split at 1530 cm^{-1}. This band partly overlaps with the absorption of aromatic ring vibrations. The band at 1370 cm^{-1} can be assigned to the so-called "umbrella" deformation of methyl groups from neopenthyl glycol and POSS. The bands at 1120 cm^{-1} and 840 cm^{-1} come from asymmetrical and symmetrical stretching vibrations of Si—O—Si group. In addition to the bands associated with the Si—O—Si vibration, also reflectance of polyester resin and polyisocyanate was found (1090 cm^{-1} C—O—C stretching; 1260 cm^{-1} asymmetrical C=O and O—CH_2 stretching and 1230 cm^{-1} C—N stretching (amide III band)). The band at 1090 cm^{-1} obscured band associated with the Si—O—Si bond at 1120 cm^{-1}. The out-of-plane (rocking) weak band of —CH_2— linear structure from POSS, IPDI and resin was visible at 728 cm^{-1}.

3.4. Surface free energy

In order to find the values of surface free energy (SFE), wetting angles were measured for two model liquids: water and diiodomethane. Water (bipolar liquids) form big drops on the coating surface (within 93.7–111.1° for the series of coatings

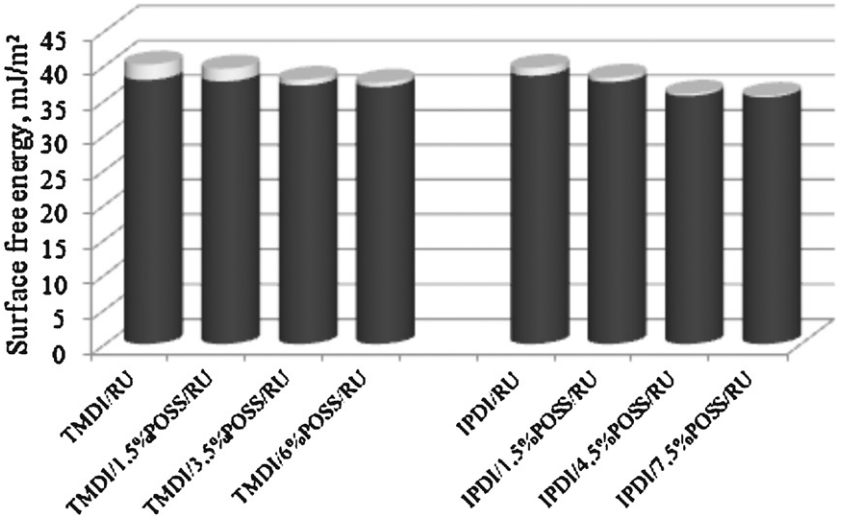

Fig. 7. Comparison values of the surface free energy for the studied coatings.

obtained from TMDI as well as within 89.9–100.5° for IPDI coatings) (Table 2), while much lower wetting angle values are specific for diiodomethane (non-polar liquid), from 41.1° to 58.2° (TMDI series) and from 40.2° to 48.8° (IPDI series). As results from the data presented in Fig. 7, the surface free energy values for the studied polyurethane coatings fall within the range of 35.6–40.1 mJ/m^2. These values classify the coatings in question as medium-polarity ones. The obtained data suggest that a major contribution to the total surface energy is made by the "amount" of dispersion interactions, which is quantitatively expressed by the parameter γ_S^d, and which is dependent on the structure of macromolecules. Polar interactions control the SFE value to a small degree only. The quantitative contribution from γ_S^p never exceeds 5.5%.

The SFE values for the POSS containing coatings were lower than for the unmodified coatings. A decrease in SFE with POSS content was observed. An increase of POSS content in the coating coincides with a decrease in the contribution of the polar component of SFE and an increase in the contribution of the dispersive component. This fact is an evidence of the water-repellent effects on the surfaces of the coatings, derived from non-polar POSS particles.

3.5. Thermogravimetric analysis (TGA)

The thermograms of IPDI series coatings were presented in Fig. 8. The thermograms include the transformations which take place during hardening and thermal decomposition processes. The sample mass loss in the temperature range of 120–220 °C is a consequence of the polyisocyanate unblocking reaction. The greatest mass loss in the sample unmodified with POSS results from the larger content of the blocking agent (ε-caprolactam) in this sample. During the synthesis of the modified samples some isocyanate groups of polyisocyanate reacted with POSS therefore the amount of ε-caprolactam used for blocking was smaller. The second stage in the temperature range of 250–350 °C can be connected with the degradation of the segments originating from polyisocyanate (decomposition of biuret and urea bonds) and was shifted to higher temperature on the addition of POSS. The next stage (in the temperature over 370 °C) is attributed to the degradation of the polyester resin segments and leads to the total degradation of the sample. During the decomposition process of POSS modified coatings, we can observe an improvement in the thermal stability at the temperature up to 350 °C as well.

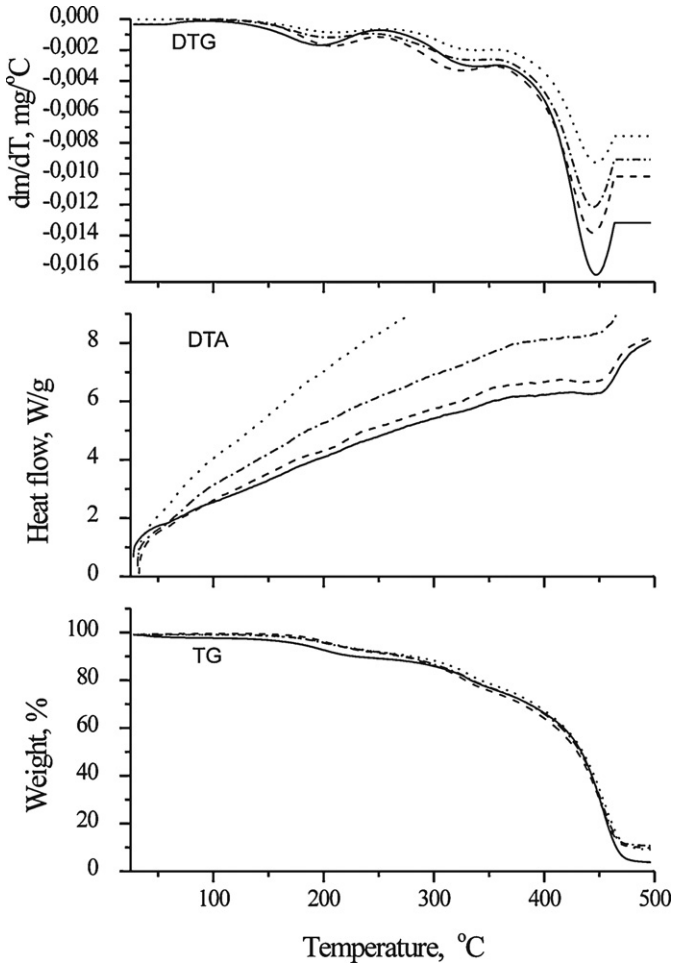

Fig. 8. DTG, DTA and TG thermograms for sample IPDI/RU (—), IPDI/1.5%POSS/RU (···), IPDI/4.5%POSS/RU (– – –) and IPDI/7.5%POSS/RU (- - -).

3.6. Performance properties of powder coatings

The thickness of coating layer significantly impacts such properties of the coatings as: hardness, impact strength and adhesion

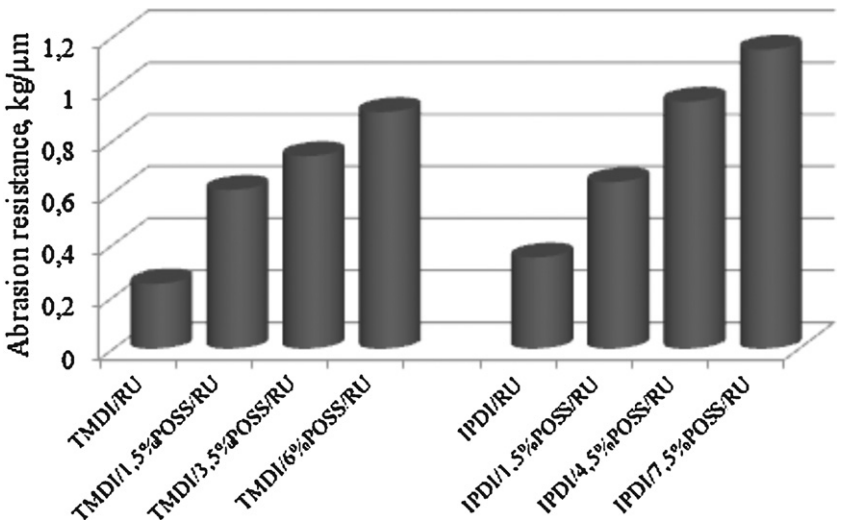

Fig. 9. Comparison values of the abrasion resistance for the studied coatings.

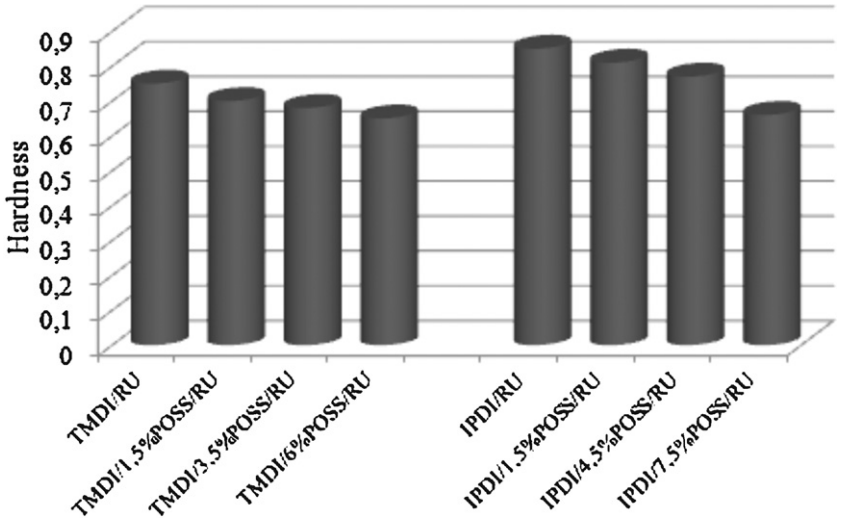

Fig. 10. Comparison values of the hardness for the studied coatings.

resistance. The mechanical properties improve with the decreasing thickness. The obtained coatings have the thickness of up to 90 μm (Table 2), which matches the range recommended by relevant standards.

Abrasion resistance of the coatings increases with the contents of POSS in the coating (Fig. 9). This is caused by the migration of POSS on the surface of the coating. The notable increase in abrasion resistance results from the higher energy of Si—O—Si (550 kJ/mol) and Si—C (369 kJ/mol) bonds occurring in POSS in comparison with the energy of C—C (334 kJ/mol), C—O (340 kJ/mol) and N—C (335 kJ/mol) bonds present in unmodified coatings.

In order to make sure that coating provides effective protection of the substrate against impacts of external environment and has good qualities as decorative finishing it is essential that its adhesion force is adequate. Indeed, the obtained coatings have the required adhesion to steel surface (Table 2). In the 0–5 point scale they have the best adhesion level (0).

Relative hardness of the studied coatings measured in a comparison with glass sheets is very good (Fig. 10). An increase in POSS content coincides with a decrease in hardness, which results from higher chain mobility of the POSS molecules. The Si—O—Si bond angle is much larger (approximately 143°), than the usual tetrahedral value (110°) [31].

Measurement of impact strength involved specifying the maximum height from which a 1-kg weight fell onto a coated panel without causing mechanical damage to the coating. The obtained coatings were found to have very good resistance to impact. They were not damaged by an impact of a weight falling from the maximum height.

The coatings obtained with a use of IPDI diisocyanate are characterized by generally better hardness and abrasion resistance if compared with the similar coatings synthesized from TMDI. This is due to the more rigid cycloaliphatic structure of IPDI in comparison with aliphatic TMDI.

4. Conclusions

The process of biurethization of IPDI and TMDI by means of formic acid, followed by an addition of POSS and ε-caprolactam allowed for synthesizing blocked polyisocyanates which in their structure contained POSS particles. On the basis of the synthesis reactions, it was concluded that the optimum conditions for

obtaining blocked polyisocyanates containing POSS particles include a four-stage process carried out in the presence of two catalysts: dibuthyltin dilaurate and triethylamine, in a nitrogen atmosphere and an appropriate temperature (within a range from 75 °C for stage I, 140 °C for stage II and 65 °C for stage III and IV). The time of the synthesis of blocked polyisocyanates depends on the chemical structure of diisocyanate. It is shorter for aliphatic TMDI.

An analysis of FT-IR and magnetic nuclear resonance spectra allowed for confirming the expected structure of the polyisocyanates and made it possible to rule out the presence of by-products: carbodiimide, isocyanurate and uretdione. The lack of bands from isocyanate groups in FT-IR and ^{13}C NMR spectra (at 2264 cm^{-1} and at 124 ppm) is an evidence for complete conversion of diisocyanates. The shift of the signals originating from methyl and methylene groups of POSS towards the higher ppm values observed in ^{1}H and ^{13}C NMR spectra, is an evidence that the POSS particles have been built into the structure of polyisocyanates.

The modern confocal microscopy made the 3D visualization of the coating surfaces possible, and the increased roughness after incorporation of POSS particles was observed. Reflection infrared spectra of the coatings confirmed the presence of the POSS on their surface (the bands from Si—O—Si bonds at 1120 cm^{-1} and 840 cm^{-1}).

On the basis of the thermogravimetric analysis results, there was a visible increase in the thermal stability of biuret and urea bonds (in the temperature range of 250–350 °C) of POSS-containing coatings.

Incorporation of the POSS particles to polyurethane powder coatings, resulted in lower surface free energy values and hardness, with simultaneously higher wetting angles, roughness values and abrasion resistance. Further increase in POSS content may cause a reduction in surface free energy and hardness as well as higher abrasion resistance and roughness. These experimental results lead to a better understanding of the surface properties and provide valuable information for the development of new polyurethane powder coating systems.

Acknowledgements

This work was supported by the Polish Ministry of Science and Higher Education under grant no. N N507 503338.

The author would like to thank Mr Ireneusz Niemiec, from NanoFocus, Oberhausen Germany, for performing confocal micrographs, Ms Dorota Naróg, Ph.D., from the Faculty of Chemistry, Rzeszów University of Technology, for taking FT-IR spectra, as well as Bayer A.G., Evonik Degussa G.m.b.H., Worlée – Chemie G.m.b.H and Zakłady Azotowe in Tarnów – Mościce S.A. for sending free samples of raw materials.

References

[1] D.B. Cordes, P.D. Lickiss, F. Rataboul, Chem. Rev. 110 (2010) 2081–2173.
[2] B. Janowski, K. Pielichowski, Polymer 53 (2008) 87–166.
[3] C. Hartmann-Thompson, Applications of Polyhedral Oligomeric Silsesquioxanes Advances in Silicon Science, vol. 3, Springer, Heidelberg, 2011.
[4] K. Pielichowski, J. Njuguna, B. Janowski, J. Pielichowski, Adv. Polym. Sci. 201 (2006) 225–296.
[5] G. Li, L. Wang, H. Ni Jr., C.U. Pittman, J. Inorg. Organomet. Polym. 11 (2001) 123–154.
[6] P.A. Wheeler, R. Misra, R.D. Cook, S.E. Morgan, J. Appl. Polym. Sci. 108 (2008) 2503–2508.
[7] E.S. Cozza, O. Monticelli, E. Marsano, Macromol. Mater. Eng. 295 (2010) 791–795.
[8] R. Misra, R.D. Cook, S.E. Morgan, J. Appl. Polym. Sci. 115 (2010) 2322–2331.
[9] L. Ricco, S. Russo, O. Monticelli, A. Bordo, F. Bellucci, Polymer 46 (2005) 6810–6819.
[10] H. Liu, S. Zheng, Macromol. Rapid Commun. 26 (2005) 196–200.
[11] K. Madhavan, B.S.R. Reddy, J. Appl. Polym. Sci. 113 (2009) 4052–4065.
[12] S. Turri, M. Levi, Macromol. Rapid Commun. 26 (2005) 1233–1236.
[13] J. Tan, Z. Jia, D. Sheng, X. Wen, Y. Yang, Polym. Eng. Sci. 51 (2011) 795–803.
[14] M. Oaten, N.R. Choudhury, Macromolecules 38 (2005) 6392–6401.
[15] I. Jerman, M. Koželj, B. Orel, Sol. Energy Mater. Sol. Cells 94 (2010) 232–245.
[16] E. Devaux, M. Rochery, S. Bourbigot, Fire Mater. 26 (2002) 149–154.
[17] R.H. Fernando, L.-P. Sung, Nanotechnology in coatings, ACS, Washington, 2009.
[18] F.E. Stagg, Analyst 71 (1966) 557–571.
[19] M. Żenkiewicz, Adhezja i modyfikowanie warstwy wierzchniej tworzyw wielkocząsteczkowych, WNT, Warsaw, 2000.
[20] European Committee for Standarization, Paints and Varnishes – Determination of Film Thickness, EN ISO 2808:1997, Brussels.
[21] Polish Committee for Standarization, Paints and Varnishes – Determination of Abrasion Resistance of Coatings, PN-76/C-81516, Warsaw.
[22] Polish Committee for Standarization, Paints and Varnishes – Pendulum Damping Test, PN-EN ISO 1522:2008, Warsaw.
[23] Polish Committee for Standarization, Paints and Varnishes – Cross-cut Test, PN-EN ISO 2409:1994, Warsaw.
[24] Polish Committee for Standarization, Paints and Varnishes – Rapid Deformation (Impact Resistance) Tests – Part 2. Falling-weight Test, Small Area Identer, PN-EN ISO 6272:2011, Warsaw.
[25] B. Pilch-Pitera, J. Appl. Polym. Sci. 124 (2012) 3302–3311.
[26] E.A. Murillo, B.L. Lopez, W. Brostow, J. Appl. Polym. Sci. 124 (2012) 3592–3599.
[27] G. Socrates, Infrared and Raman Characteristic Group Frequencies: Tables and Charts, Wiley, New York, 2004.
[28] A. Lapprand, F. Boisson, F. Delolme, F. Méchin, J.-P. Pascault, Polym. Degrad. Stab. 90 (2005) 363–373.
[29] Q.-W. Lu, T.R. Hoye, C.W. Macosco, J. Polym. Sci. A: Polym. Chem. 40 (2002) 2310–2328.
[30] A. Prabhakar, D.K. Chattopadhyay, B. Jagadeesh, K.V.S.N. Raju, J. Polym. Sci. A: Polym. Chem. 43 (2005) 1196–1209.
[31] J.E. Mark, Acc. Chem. Res. 37 (2004) 946–953.